Available online at www.sciencedirect.com
ScienceDirect
Physica E 38 (2007) 148–151
PHYSICA E
www.elsevier.com/locate/physe

Visible photoluminescence from silicon nanoclusters embedded in silicon nitride films prepared by remote plasma-enhanced chemical vapor deposition

A. Benami[a], G. Santana[a,*], B.M. Monroy[a], A. Ortiz[a], J.C. Alonso[a], J. Fandiño[b], J. Aguilar-Hernández[c], G. Contreras-Puente[c]

[a]Instituto de Investigaciones en Materiales, Universidad Nacional Autónoma de México, 70-360, Coyoacán 04510, DF México
[b]Instituto de Física, Universidad Nacional Autónoma de México, A.P. 20-364, Coyoacán 01000, DF México
[c]Escuela Superior de Física y Matemáticas del IPN; Ed. 9, UPALM 07738, DF México

Available online 31 December 2006

Abstract

The photoluminescence (PL) of silicon nanoclusters embedded in silicon nitride films grown by remote plasma-enhanced chemical vapor deposition at 200 °C, using mixtures of $SiCl_4/H_2/Ar/NH_3$ is investigated. It was found that the color and the intensity of the PL of the as-grown samples depend on the H_2 flow rate, and there is an optimum flow for which a maximum luminescence is obtained. A strong improvement of the PL intensity and change in color was obtained with annealing treatments in the range of 500–1000 °C. The changes in the composition, structure and optical properties of the films, as a function of H_2 flow rate and thermal treatments, were studied by means of Fourier-transform infrared spectroscopy, X-ray photoelectron spectroscopy, ellipsometry and ultraviolet–visible transmission measurements. We conclude that the PL can be attributed to quantum confinement effect in silicon nanoclusters embedded in silicon nitride matrix, which is improved when a better passivation of the nanoclusters surface is obtained.
© 2007 Elsevier B.V. All rights reserved.

PACS: 61.72.Ww; 78.55.−m; 81.15.Gh; 61.72.Tt

Keywords: Nanoclusters; Photoluminescence; RPECVD; Silicon

1. Introduction

There is much interest in obtaining Si-based luminescent materials, compatible with the present silicon technology, to be used in the development of integrated optoelectronic devices. In principle, due to its indirect band gap, bulk silicon is a less suitable material for the fabrication of light-emitting devices than the direct band gap semiconductors. However, nanometer-sized silicon particles show unique changes in their electronic structure and optical properties, which convert them into better light emitters. Photoluminescent silicon nanocrystals and/or silicon nanoclusters embedded in insulating silicon-based thin films have been produced by several techniques, such as, plasma-enhanced chemical vapor deposition (PECVD) [1–3], PECVD and thermal annealing [4], electron gun evaporation [5], Si/Er ion implantation [6]. In particular, the formation of silicon nanocrystals embedded in silicon-rich-silicon nitride (SiN_x) films prepared by PECVD techniques has proved to be advantageous for obtaining strong tunable and/or multi-color emission in the visible region, which can be controlled by varying the growth conditions [1–3].

In this work, we report the photoluminescence (PL) from silicon nanoclusters embedded in SiN_x films prepared by the remote plasma-enhanced chemical vapor deposition (RPECVD) technique from $SiCl_4/NH_3/H_2$ mixtures. We also investigate the influence of hydrogen dilution on the structure, optical and luminescent properties of the films, and discuss the PL characteristics in terms of the quantum confinement model.

*Corresponding author. Tel.: +52 55 56 22 46 06; fax: +52 55 56 16 12 51.
E-mail address: gsantana@iim.unam.mx (G. Santana).

1386-9477/$ - see front matter © 2007 Elsevier B.V. All rights reserved.
doi:10.1016/j.physe.2006.12.047

2. Experimental details

The films were deposited on high-resistivity monocrystalline silicon n-type (1 0 0), using the RPECVD system described elsewhere [7]. Before deposition, the silicon substrates were cleaned by a standard procedure for removing contaminants and the surface native oxide [8], and finally rinsed in deionized water and blown dry with ultrapure nitrogen gas. High-purity $SiCl_4$, NH_3 and H_2 were used as precursor gases. The flow rate ratio of $[SiCl_4]/[NH_3]$ was kept constant at 0.2 sccm, while the hydrogen flow rate was varied from 0 to 60 sccm. For each flow rate of H_2, a flow rate of Ar was added to adjust the working pressure to 40 Pa. The RF power, and substrate temperature were kept constant at 200 Watt and 200 °C, respectively. Films with different deposition rates were obtained, depending on the H_2 flow rate (see Table 1). The deposition time was adjusted for obtaining films with thickness about ~1000 nm. After deposition, pieces of each sample were annealed in nitrogen atmosphere for 1 h in the range from 500 to 1000 °C. The refractive index and thickness of the films were measured by ellipsometry using a Gaertner L117 Ellipsometer equipped with a He–Ne laser ($\lambda = 632.8$ nm) and an incidence angle of 70°. The chemical bonding behavior was analyzed by means of a Fourier-Transform Infrared (FTIR) spectrophotometer (Nicolet-210). X-ray photoelectron spectroscopy (XPS) analysis of the composition was performed with the aid of a VG Microtech Multilab ESCA 2000 system. PL studies were carried out at room temperature in a conventional PL system described in detail elsewhere [9]. A 10 mW He–Cd laser (325 nm) was used as excitation source. All the spectra were corrected taking into account the spectral response of the system.

3. Results and discussion

Fig. 1 shows the room-temperature PL spectra of the as-grown samples as a function of H_2 flow rate. It can be seen that the PL of all the samples is in the visible range. The PL intensity increases strongly as the H_2 flow rate increases from 0 to 20 sccm, and then decreases for further increase of the H_2 flow rate. Although the structure of the spectra

Table 1
Flow rate of H_2, growth rate, refractive index and relative composition of as-grown and annealed silicon nitride films deposited by RPECVD

Sample	Flow rate H_2	Growth rate (nm/min)	N/Si	O/Si	Cl/Si	Refractive index
M56	10	31.2	0.55	0.52	0.14	1.93
M56T1	10	—	0.57	0.64	0.1	—
M63	20	34	0.54	0.19	0.21	1.836
M63T1	20	—	0.56	0.53	0.11	—
M53	40	30.7	0.57	0.19	0.20	1.936
M53T1	40	—	0.61	0.32	0.14	—
M54	60	29.2	0.62	0.20	0.16	1.929
M54T1	60	—	0.65	0.55	0.11	—

Sample names ending with T1 refer to samples after annealing at 1000 °C.

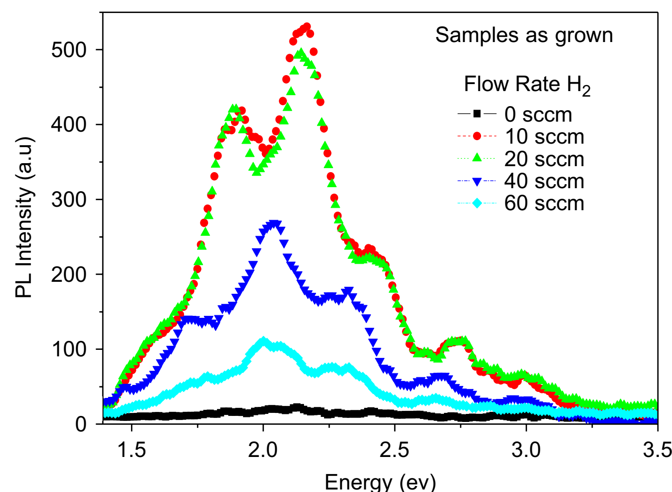

Fig. 1. Room-temperature PL spectra of silicon nanocluster for as-grown samples deposited at different H_2 flow rates.

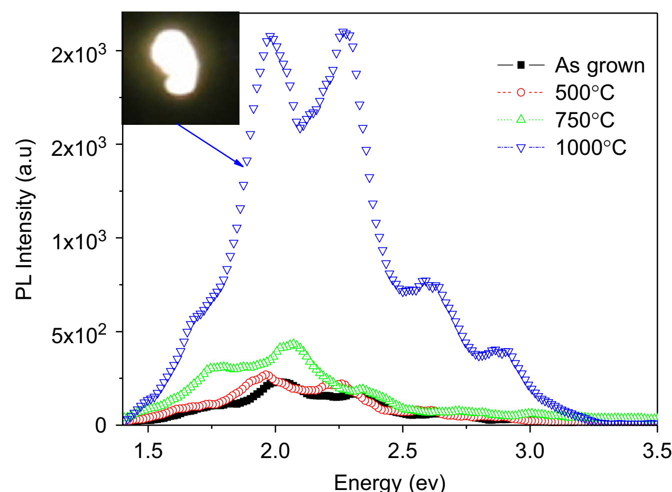

Fig. 2. Room-temperature PL spectra of the sample grown with 40 sccm of H_2, and annealed at different temperatures. The inset in the figure shows the PL spot with the corresponding emission color, as seen with the naked eye in a bright room.

depends on the H_2 flow rate, the color of the emission does not change significantly with the hydrogen dilution used during deposition. Fig. 2 shows the PL behavior of the sample deposited with a H_2 flow rate of 40 sccm, as a function of the annealing temperature. It can be seen that there are no significant changes in the PL intensity and color for annealing temperatures up to 750 °C. However, an improvement by almost one order of magnitude in the PL intensity and a transformation of color, from greenish to white, occur when the annealing temperature is 1000 °C. The inset in Fig. 2 shows the white PL spot, as seen with the naked eye in a bright room.

Fig. 3 shows the FTIR of the as-grown silicon nitride films deposited under different H_2 flow rates. All the spectra show a main absorption band located at ~864 cm^{-1} which is assigned to the stretching vibration mode of Si–N

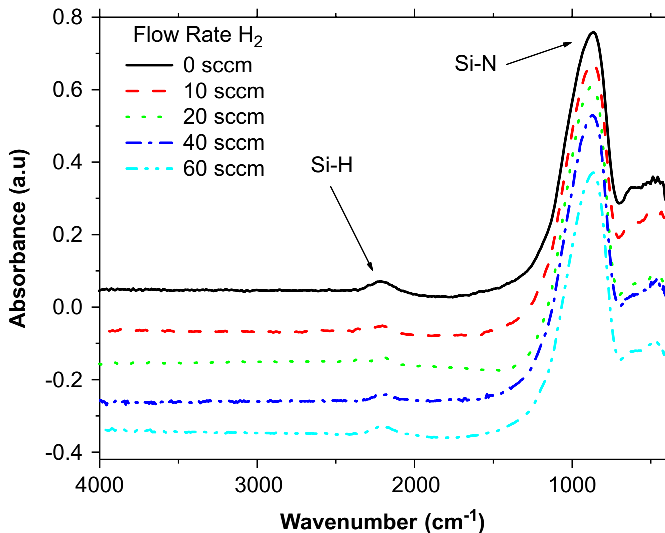

Fig. 3. FTIR spectra of as-grown samples as a function of H_2 flow rate.

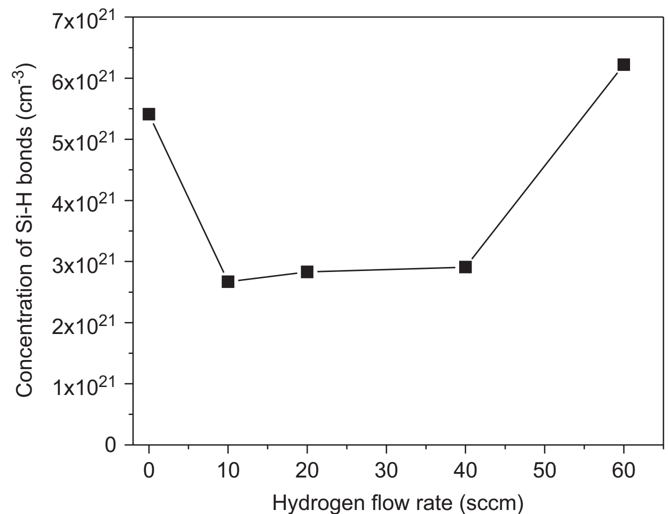

Fig. 4. Calculated concentration of Si–H bonds in the films as a function of hydrogen flow rate.

bonds, and two other small peaks positioned at ~2209 and ~462 cm^{-1}, which can be associated to Si–H stretching mode vibrations and Si atom breathing vibrations in silicon nitride, respectively [11]. There is no evidence for any absorption associated with N–H vibrations, which would be located at ~3335 cm^{-1} (stretching mode) and 1175 cm^{-1} (bending mode) [11]. The presence of Si–Cl bonds was also difficult to observe from the FTIR spectra.

Although there is no significant change in the position of the absorption band assigned to Si–N and Si–H bonds, as a function of H_2 flow rate, the area under these peaks, which is proportional to the concentration of the corresponding bonds, does suffer some small changes with the changes in the hydrogen flow rate.

The concentration of Si–H bonds in the films was calculated from the area of the FTIR Si–H absorption band using the formula:

$$[\mathrm{Si{-}H}] = \frac{2.303}{d} K \int A(\omega)\,\mathrm{d}\omega, \qquad (1)$$

where [Si–H] is the concentration of Si–H bonds, $A(\omega)$ is the absorbance produced by the corresponding band as a function of the wave number ω, d is the thickness of the film, and $K = 7.1 \times 10^{16}\,\mathrm{cm}^{-1}$ [10–12]. As Fig. 4 shows the concentration of Si–H bonds in the as-grown films is below $7 \times 10^{21}\,\mathrm{cm}^{-3}$, and it decreases with the increase of H_2 flow rate from 0 to 10 sccm, and becomes approximately constant in the interval from 10 to 40 sccm. Over 40 sccm, the concentration of Si–H bonds increases with increments in the H_2 flow rate. The behavior of the amount of Si–H bonds and the trends in the XPS composition of the films as a function of H_2 flow rate shown in Table 1, can be explained in terms of the deposition chemistry and stability of the films [7,10]. Films deposited without hydrogen result with many chlorine atoms incorporated and they hydrolyze easily when exposed to the ambient atmosphere [7,10]. This hydrolization process can remove Cl atoms from the film and favors the incorporation of oxygen and hydrogen in its network. On the other hand, the main effect of adding hydrogen (10–40 sccm) during deposition is the reduction of Cl incorporated in the films through the formation of HCl, which improves the stability of the as-grown films. At higher H_2 flow rates, the excess of H atoms will favor the incorporation of Si–H bonds in the films. From UV–visible measurement for the films grown on silica fused substrates, the optical band gap (E_g) was calculated using the Tauc formula, $(\alpha h\nu)^{1/2} = B(h\nu - E_g)$, and it was between 2.4 and 3.0 eV, which is characteristic of silicon-rich silicon nitride [13]. The refractive indices of these films, which were between 1.83 and 1.93, are consistent with these compositions [3].

The origin of the PL from silicon nanostructures is often associated to quantum confinement effects [1–3]. According to this model, the position of the PL energy peak is inversely proportional to the square of the average size of the silicon nanoclusters (nc-Si). Meanwhile, the PL intensity increases with the density of nc-Si and with a better passivation. According to the IR spectra in Fig. 1, and the data of XPS composition (Table 1), the silicon nitride films contain important amounts of oxygen, chlorine and hydrogen (in fact, they could be called silicon-rich silicon oxynitride). Therefore, the nc-Si with intense luminescence embedded in the insulating matrix can be passivated with nitrogen, chlorine, oxygen and hydrogen atoms, in amounts that depend on the H_2 flow rate. Our results indicate that the best passivation is obtained for H_2 flow rates in the range from 10 to 40 sccm. Since in this range of H_2 dilution the incorporation of Si–H bonds in the films (see Fig. 5) is minimal, we can conclude that in these cases the passivation is mostly provided by N, O and Cl atoms (see Table 1). The fact that the PL color does not change significantly with the H_2 flow rate indicates that the average size of nc-Si is not sensitive to H_2 dilution. As can be seen in Fig. 5, after the thermal

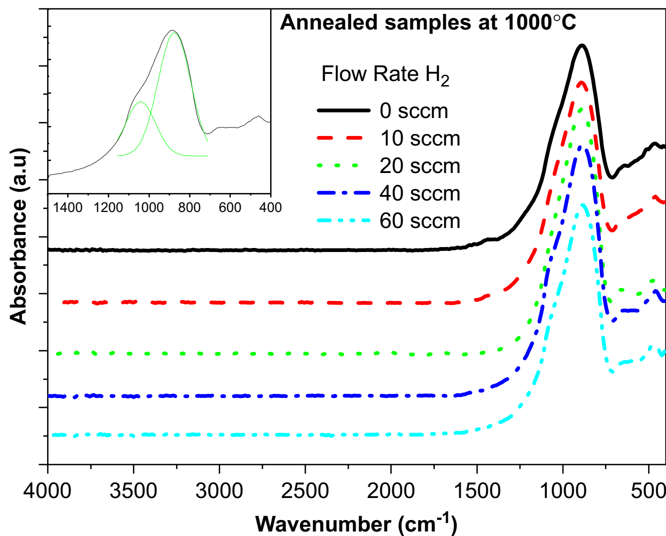

Fig. 5. FTIR spectra of annealed samples at 1000 °C deposited at different H_2 flow rate. The inset shows the evidence of the Si–O shoulder.

annealing process the amount of Si–H bond in all these films is reduced to undetectable limits, and a weak shoulder appears at $\sim$1075 cm^{-1}, which is associated with Si–O stretching mode (see inset in Fig. 5), indicating that the annealed films suffered some oxidation. The XPS composition data shown in Table 1 show that, in addition to the oxidation of the films, they also lose certain amount of chlorine atoms after annealing.

Thus, the improvement in the PL intensity of the sample prepared with 40 sccm of H_2 after annealing at 1000 °C, shown in Fig. 2, means that the rupture of Si–H and Si–Cl bonds and the effusion of H and Cl atoms from the film leaves silicon dangling bonds, which are then saturated by N and O atoms from the matrix, and also promote the formation of new and smaller silicon nanoclusters [3,4].

4. Conclusions

We conclude that the color and the intensity of the PL of the as-grown samples depend strongly on the H_2 flow rate and the PL intensity can be attributed to quantum confinement effect in silicon nanoclusters embedded in silicon nitride matrixes. The blueshift and improvement in the PL intensity occur when new nanoclusters are formed and a better passivation surface is obtained with the annealing treatment.

Acknowledgements

We acknowledge the technical assistance of L. Huerta, M.A. Canseco, C. Flores J. Camacho, S. Jimenez, and partial financial support for this work from CONACyT-México, under project 47303-F, PAPIIT-UNAM under project IN-109803 and PAPIIT-UNAM under project IN-114406-2. Abellah Benami is thankful to DGEP-UNAM for the Scholarship.

References

[1] Z. Pei, H.L. Hwang, Appl. Surf. Sci. 212 (2003) 760.
[2] B.H. Kim, C.H. Cho, T.W. Kim, N.M. Park, G.Y. Sung, S.J. Park, Appl. Phys. Lett. 86 (2005) 011908.
[3] G. Santana, B.M. Monroy, A. Ortiz, L. Huerta, J.C. Alonso, J. Fandiño, L. Aguilar-Hernández, E. Hoyos, F. Cruz-Gandarilla, G. Contreras-Puentes, Appl. Phys. Lett. 88 (2006) 041916.
[4] F. Iacona, C. Bongiorno, C. Spinella, J. Appl. Phys. 95 (2004) 3723.
[5] L.Y. Chen, W.H. Chen, F.C.N. Hong, Appl. Phys. Lett. 86 (2005) 193506.
[6] X.Q. Cheng, J.M. Sun, R. Kogler, W. Skorupa, W. Moller, S. Prucnal, Vacuum 78 (2005) 667.
[7] J.C. Alonso, R. Vazquez, A. Ortiz, V. Pankov, E. Andrade, J. Vac. Sci. Technol. A16 (1998) 3211.
[8] J. Fandiño, G. Santana, L. Rodríguez-Fernández, J.C. Cheang-Wong, A. Ortiz, J.C. Alonso, J. Vac. Sci. Technol. A 23 (2005) 248.
[9] J. Aguilar-Hernández, G. Contreras-Puente, J.M. Figueroa-Estrada, O. Zelaya-Angel, Jpn. J. Appl. Phys. 33 (1994) 37.
[10] G. Santana, J. Fandiño, A. ortiz, J.C. Alonso, J. Non-Cryst. Solids 351 (2005) 922.
[11] D.V. Tsu, G. Lucovsky, M.J. Mantini, Phys. Rev. B (1986) 7069.
[12] W.A. Lanford, M.J. Rand, J. Appl. Phys. 49 (1978) 2473.
[13] A. Shih, S.H. Yeh, S.C. Lee, T.R. Yang, J. Appl. Phys. 89 (2001) 5355.